Validation of Static and Dynamic SGS models for LES of Compressible Flows

By S. Ryu, I. Bermejo-Moreno AND G. Iaccarino

Center for Turbulence Research, Stanford University, 488 Escondido Mall
Stanford, CA 94305, USA

We developed two subgrid-scale (SGS) eddy-viscosity models: pseudo strain-acceleration based SGS model and SGS Reynolds stress based dynamic Vreman model. Because the two models were derived under assumptions of incompressible flows, validations of the models in the compressible flow regime are required to confirm their global applicability to LES. In this paper, the proposed two SGS models are validated in the LES of wall-bounded compressible flows: compressible channel flow at Re_τ=221 with Ma=1.5 and Re_τ=556 with Ma=3.0. Moreover, to assess their performance, LES with the dynamic Smagorinsky model (DSM) and the Vreman model are also performed in the same flow configurations. Finally, we will show in the future that the proposed two models are applicable for physically complex flows by a wall-modeled large eddy simulation (WMLES) of geometrically induced shock-turbulent-boundary-layer interactions (STBLI).

1. Introduction

Numerical simulations of turbulent flows in engineering applications are challenging, especially in the high Reynolds number regime. As an alternative to direct numerical simulation (DNS), large eddy simulation (LES) is widely used as an efficient method computationally less costly than DNS. However, LES requires a closure of the unresolved turbulent stresses, which are expressed as

$$\tau_{ij} = \overline{u_i u_j} - \overline{u}_i \overline{u}_j \tag{1.1}$$

where $\overline{(.)}$ is a filtered quantity. To improve the accuracy of LES, many researchers have studied subgrid-scale (SGS) turbulence modeling to accurately reproduce the SGS stresses generated by a filtering process. SGS closures are typically defined in terms of an eddy viscosity mirroring the effect of the molecular viscosity, in a form

$$\tau_{ij} - \frac{1}{3}\tau_{kk}\delta_{ij} = -2\nu_t \overline{S}_{ij} \tag{1.2}$$

where ν_t is the SGS eddy viscosity and $\overline{S}_{ij} = (1/2)(\partial \overline{u}_i/\partial x_j + \partial \overline{u}_j/\partial x_i)$ is the filtered strain-rate tensor.

Since the Smagorinsky model was proposed based on a magnitude of the strain-rate tensor in Ref. [1], various SGS eddy viscosity models have been developed. The main weakness of the Smagorinsky model is that it does not capture the turbulence damping near a solid wall, i.e., the eddy viscosity does not decay towards the wall. Moreover, it does not vanish in simple laminar flows. Later, Vreman (2004) [2] developed an eddy

viscosity model which satisfies the condition that the SGS dissipation theoretically vanishes in various laminar shear flows by means of algebraic relations among components of the velocity gradient tensor. However, Nicoud *et al.* (2011) [3] theoretically demonstrated that the asymptotic wall behavior of the Vreman model is unable to capture the correct cubic dependency with the distance y from the wall , i.e., the eddy viscosity of the Vreman model decays as order $O(y)$ near the wall. To improve the Smagorinsky model, Germano *et al.* (1991) [4] proposed the dynamic Smagorinsky model (DSM), where the model coefficient is determined from scale invariance between SGS stresses at two filter levels and resolved turbulent stresses. However, plane-averaging with respect to homogeneous direction(s) in a computation domain and/or *ad hoc* clipping are needed to avoid numerical instability. Consequently, the applicability of the original DSM has been limited to the LES of turbulent flows with statistically homogeneous direction(s).

1.1. *Pseudo strain-acceleration based model (PSA-model)*

In the first step of the development of the PSA-model, using off-diagonal components of the strain-rate tensor, the PSA tensor R_{ij} can be defined as

$$R_{ij} = \gamma_i \frac{\partial u_j}{\partial x_k}\delta_{jk} = \begin{pmatrix} \gamma_1\frac{\partial u}{\partial x} & \gamma_1\frac{\partial v}{\partial y} & \gamma_1\frac{\partial w}{\partial z} \\ \gamma_2\frac{\partial u}{\partial x} & \gamma_2\frac{\partial v}{\partial y} & \gamma_2\frac{\partial w}{\partial z} \\ \gamma_3\frac{\partial u}{\partial x} & \gamma_3\frac{\partial v}{\partial y} & \gamma_3\frac{\partial w}{\partial z} \end{pmatrix} \tag{1.3}$$

where $\boldsymbol{\gamma} = (\gamma_1, \gamma_2, \gamma_3) = (S_{23}, S_{13}, S_{12})$. It is notable that the magnitude of the second order PSA tensor R_{ij} reflects the spatial variation of the strain-rate in turbulent flows. Thus, it could be more appropriate to capture the three dimensionality of turbulence than the magnitude of the strain-rate tensor. To investigate the behavior of R_{ij} with respect to the wall-normal distance close to the wall, the velocity vector close to the wall is expanded in polynomial form with respect to the wall-normal coordinate y, as below:

$$u = a_1 y + a_2 y^2 + a_3 y^3 + O(y^4) \tag{1.4a}$$

$$v = b_2 y^2 + b_3 y^3 + O(y^4) \tag{1.4b}$$

$$w = c_1 y + c_2 y^2 + c_3 y^3 + O(y^4) \tag{1.4c}$$

where the coefficients a_i, b_i, c_i are functions of the other coordinates x, z and time t. Note that b_1 is equal to zero to satisfy the incompressible continuity equation close to the solid wall. Then, the leading order of each component of the R_{ij} tensor is determined by substituting (1.4*a*), (1.4*b*) and (1.4*c*) into (1.3):

$$R_{ij} = \begin{pmatrix} O(y) & O(y) & O(y) \\ O(y^2) & O(y^2) & O(y^2) \\ O(y) & O(y) & O(y) \end{pmatrix} \tag{1.5}$$

An operator $(\overline{R}_{ij}\overline{R}_{ij})^{\frac{3}{2}}$ is chosen with the exponent $3/2$ to satisfy the cubic wall-behavior [$(\overline{R}_{ij}\overline{R}_{ij})^{\frac{3}{2}} \sim O(y^3)$]. This operator has a unit of $1/sec^6$, which is the same as those of the operator $(s^d_{ij}s^d_{ij})^{3/2}$ (Note that the tensor s^d_{ij} is a traceless symmetric part of the square of the velocity gradient tensor) of the WALE model [5]. Thus, the same approach used in the WALE model is applied to scale the operator keeping the cubic behavior, i.e., the denominator $(\overline{S}_{ij}\overline{S}_{ij})^{5/2}$ is chosen in our model because it has a unit $1/sec^5$ with order $O(1)$ in Ref. [5]. Based on the above observations, we propose a SGS eddy

viscosity model as below:

$$\nu_t = (c_r\Delta)^2 \frac{(\overline{R}_{ij}\overline{R}_{ij})^{\frac{3}{2}}}{(\overline{S}_{ij}\overline{S}_{ij})^{\frac{5}{2}}} \tag{1.6}$$

where $c_r = 1.3$ is a model coefficient, and Δ is a characteristic SGS length scale $\Delta = (\Delta_1\Delta_2\Delta_3)^{1/3}$. The $\overline{R}_{ij}$ and $\overline{S}_{ij}$ are traceless with the filtered velocity components. The model coefficient 1.3 was empirically determined by LES of freely decaying isotropic turbulence and incompressible turbulent channel flow at $Re_\tau = 395$.

1.2. *SGS Reynolds stress based dynamic Vreman model (RD-Vreman model)*

We developed a dynamic procedure based on the Reynolds decomposition and its filtered relation which are written as below:

$$u_i = \bar{u}_i + u_i' \tag{1.7}$$

$$\bar{u}_i = \overline{\bar{u}_i + u_i'} = \bar{\bar{u}}_i + \bar{u}_i' \tag{1.8}$$

where $\overline{\overline{(.)}}$ is the twice-filtered quantity. The two relations above are used to derive a relation of identity between SGS Reynolds stress and SGS eddy viscosity. First, we derive the incompressible Navier-Stokes equations for the filtered SGS velocity components $\bar{u}_i'$ by inserting (1.7) into the original incompressible Navier-Stokes equation as below:

$$\frac{\partial(\bar{u}_i + u_i')}{\partial t} + \frac{\partial(\bar{u}_i\bar{u}_j + \bar{u}_i u_j' + u_i'\bar{u}_j + u_i'u_j')}{\partial x_j} = -\frac{\partial(\bar{p} + p')}{\partial x_i} + \nu\frac{\partial^2(\bar{u}_i + u_i')}{\partial x_j \partial x_j} \tag{1.9}$$

$$\frac{\partial \bar{u}_i}{\partial t} + \frac{\partial \bar{u}_i\bar{u}_j}{\partial x_j} = -\frac{\partial \bar{p}}{\partial x_i} + \nu\frac{\partial^2 \bar{u}_i}{\partial x_j \partial x_j} - \frac{\partial \tau_{ij}}{\partial x_j} \tag{1.10}$$

Then, by subtracting the filtered incompressible Navier-Stokes equation (1.10) from (1.9) the residual Navier-Stokes equations are obtained as

$$\frac{\partial u_i'}{\partial t} + \frac{\partial(\bar{u}_i u_j' + u_i'\bar{u}_j + u_i'u_j')}{\partial x_j} = -\frac{\partial p'}{\partial x_i} + \nu\frac{\partial^2 u_i'}{\partial x_j \partial x_j} + \frac{\partial \tau_{ij}}{\partial x_j} \tag{1.11}$$

where $\tau_{ij} = \overline{u_i u_j} - \bar{u}_i\bar{u}_j$. Then, (1.11) can be rewritten after filtering the whole equation and then arranging it as

$$\frac{\partial \bar{u}_i'}{\partial t} + \frac{\partial \bar{u}_i'\bar{u}_j'}{\partial x_j} = -\frac{\partial \bar{p}'}{\partial x_i} + \nu\frac{\partial^2 \bar{u}_i'}{\partial x_j \partial x_j} - \frac{\partial \alpha_{ij}}{\partial x_j} \tag{1.12}$$

Where $\alpha_{ij} = -\bar{\tau}_{ij} + \overline{\bar{u}_i u_j'} + \overline{u_i'\bar{u}_j} + (\overline{u_i'u_j'} - \bar{u}_i'\bar{u}_j')$. The filtered cross stress term $\overline{\bar{u}_i u_j'} + \overline{u_i'\bar{u}_j}$ in the definition of α_{ij} was modeled by Bose and Moin (2010) in Ref. [6] as $\bar{u}_i\bar{u}_j' + \bar{u}_i'\bar{u}_j$. Based on the modeling of the cross stress term, α_{ij} can be approximated as

$$\alpha_{ij} \approx -\bar{\tau}_{ij} + \bar{u}_i\bar{u}_j' + \bar{u}_i'\bar{u}_j + (\overline{u_i'u_j'} - \bar{u}_i'\bar{u}_j') \tag{1.13}$$

$$\alpha_{ij} \approx -\bar{\tau}_{ij} + \bar{u}_i\bar{u}_j' + \bar{u}_i'\bar{u}_j + \gamma_{ij} \tag{1.14}$$

where $\gamma_{ij} = \overline{u_i'u_j'} - \bar{u}_i'\bar{u}_j'$. Another form of the Navier-Stokes equation the solutions of which are filtered SGS velocity components $\bar{u}_i'$ can be derived by subtracting the twice-filtered Navier-Stokes equations (1.15) from (1.10).

$$\frac{\partial \bar{\bar{u}}_i}{\partial t} + \frac{\partial \bar{\bar{u}}_i\bar{\bar{u}}_j}{\partial x_j} = -\frac{\partial \bar{\bar{p}}}{\partial x_i} + \nu\frac{\partial^2 \bar{\bar{u}}_i}{\partial x_j \partial x_j} - \frac{\partial T_{ij}}{\partial x_j} \tag{1.15}$$

where $T_{ij} = \overline{\overline{u_i u_j}} - \bar{\bar{u}}_i \bar{\bar{u}}_j$. Then, The other version of the Navier-Stokes equations for filtered SGS velocity components is rewritten as

$$\frac{\partial \bar{u}_i'}{\partial t} + \frac{\partial(\bar{u}_i \bar{u}_j - \bar{\bar{u}}_i \bar{\bar{u}}_j)}{\partial x_j} = -\frac{\partial \bar{p}'}{\partial x_i} + \nu \frac{\partial^2 \bar{u}_i'}{\partial x_j \partial x_j} - \frac{\partial(\tau_{ij} - T_{ij})}{\partial x_j} \tag{1.16}$$

After subtracting (1.12) from (1.16), the residual equation can be arranged as:

$$\frac{\partial(\bar{u}_i' \bar{u}_j' - \bar{u}_i \bar{u}_j + \bar{\bar{u}}_i \bar{\bar{u}}_j)}{\partial x_j} = \frac{\partial(-\alpha_{ij} + \tau_{ij} - T_{ij})}{\partial x_j} \tag{1.17}$$

$$\frac{\partial(\bar{u}_i' \bar{u}_j' - \bar{u}_i \bar{u}_j + \bar{\bar{u}}_i \bar{\bar{u}}_j)}{\partial x_j} = \frac{\partial(\bar{\tau}_{ij} - \bar{u}_i \bar{u}_j' - \bar{u}_i' \bar{u}_j - \gamma_{ij} + \tau_{ij} - T_{ij})}{\partial x_j} \tag{1.18}$$

$$\frac{\partial[\bar{u}_i' \bar{u}_j' - \bar{u}_i \bar{u}_j + (\bar{u}_i - \bar{u}_i')(\bar{u}_j - \bar{u}_j')]}{\partial x_j} = \frac{\partial(\bar{\tau}_{ij} - \bar{u}_i \bar{u}_j' - \bar{u}_i' \bar{u}_j - \gamma_{ij} + \tau_{ij} - T_{ij})}{\partial x_j} \tag{1.19}$$

$$2\frac{\partial \bar{u}_i' \bar{u}_j'}{\partial x_j} = \frac{\partial(\bar{\tau}_{ij} - \gamma_{ij} + \tau_{ij} - T_{ij})}{\partial x_j} \tag{1.20}$$

$$2\bar{u}_i' \bar{u}_j' = \bar{\tau}_{ij} - \gamma_{ij} + \tau_{ij} - T_{ij} \tag{1.21}$$

where four different kinds of SGS stresses $\tau_{ij},\ \bar{\tau}_{ij},\ T_{ij}$, and γ_{ij} are modeled with a SGS eddy viscosity type as

$$\tau_{ij} - \frac{1}{3}\tau_{kk}\delta_{ij} \approx -2\nu_T \bar{S}_{ij} \tag{1.22}$$

$$\bar{\tau}_{ij} - \frac{1}{3}\bar{\tau}_{kk}\delta_{ij} \approx -2\overline{\nu_T \bar{S}_{ij}} \tag{1.23}$$

$$T_{ij} - \frac{1}{3}T_{kk}\delta_{ij} \approx -2\nu_T^t \bar{\bar{S}}_{ij} \tag{1.24}$$

$$\gamma_{ij} - \frac{1}{3}\gamma_{kk}\delta_{ij} \approx -2\nu_T^p \bar{S}_{ij}^p \tag{1.25}$$

where the three kinds of SGS eddy viscosities ν_T, ν_T^t and ν_T^p are calculated using $\bar{u}_i$, $\bar{\bar{u}}_i$, and $\bar{u}_i'$, respectively. Moreover, the traceless strain-rate tensors $\bar{S}_{ij}$, $\bar{\bar{S}}_{ij}$, and $\bar{S}_{ij}^p$ are calculated using the same components, respectively. Then, the local Vreman model coefficient $C_v^*(x,y,z,t)$ is calculated as below:

$$C_v^*(x,y,z,t) = \frac{Y_{ij}U_{ij}}{U_{mn}U_{mn}}, \tag{1.26}$$

where the traceless SGS Reynolds stress tensor is $Y_{ij} = 2[\bar{u}_i'\bar{u}_j' - (1/3)\delta_{ij}\bar{u}_k'\bar{u}_k']$ and $U_{ij} = 2\overline{\Pi \bar{S}_{ij}} - 2\Pi^p \bar{S}_{ij}^p + 2\Pi \bar{S}_{ij} - 2\Pi^t \bar{\bar{S}}_{ij}$. However, note that negative and/or excessively large model coefficients can cause numerical instability in an actual LES. Thus, a clipping with a lower and upper limit is applied. Using the clipping function, the local coefficient $C_v(x,y,z,t)$ is determined as

$$C_v = max[0, min(C_v^*, \sigma)] \tag{1.27}$$

where the upper limit σ (=0.23) is empirically determined by a parameter test on the LES of decaying isotropic turbulence.

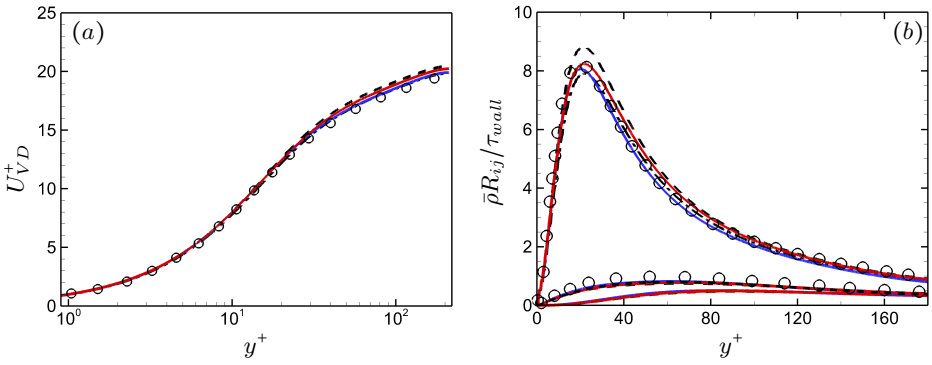

FIGURE 1. (*a*) The Van-Driest transformed mean velocity profiles at Re_τ=221 with Ma=1.5: — · — , Vreman model; — — —, dynamic Smagorinsky model; blue solid line, PSA-model; red solid line, RD-Vreman mode; ∘, DNS data in Ref. [9] (*b*) Normalized turbulent stresses (R_{11}, R_{22}, R_{33}), $\bar{\rho}R_{ij} = \overline{\rho u_i'' u_j''}$, profiles of Favre velocity fluctuations obtained with four SGS models (same as (a)).

2. Numerical method

The spatially filtered, compressible Navier-Stokes equations for LES are solved by a finite volume-based code, which is called CharLESX [7]. This solver was developed at Stanford's Center for Turbulence Research (CTR). All conserved variables are advanced using a third-order Runge-Kutta scheme with a time step corresponding to maximum CFL≈1.5. Spatial derivatives for the variables are approximated based on the second order grid-based blend of non-dissipative central and dissipative upwind fluxes. Detailed descriptions of the spatial discretization are presented by Khalighi *et al.* (2011) [8]. The essentially non-oscillatory (ENO) scheme is applied to reconstruct steep variations of flow variables. About 2.5 percentage of the total number of grid cells are reconstructed by the shock capturing scheme.

3. Results

3.1. *Compressible turbulent channel flow at Re_τ=221*

We first performed LES of compressible turbulent channel flow at Re_τ=221 and Ma=1.5. Table 1 displays the physical and grid parameters with respect to each SGS model compared with those of DNS by Foysi *et al.* [9]. The grid for LES is three and two times coarser than the DNS grid in streamwise and spanwise directions, respectively. However, wall-normal grid resolution is almost around that of DNS to clarify the differences of performance in turbulent statistics with respect to each SGS model. The bulk Reynolds numbers calculated from LES results with PSA and RD-Vreman model show good agreement with those of DNS.

Figure 1 shows the Van-Driest transformed mean velocity profiles and turbulence quantities obtained with four SGS models. The mean profiles, obtained with the PSA and RD-Vreman models, show equivalent or better performance than the established two models, DSM and Vreman model, in a whole range of wall-normal coordinate. In figure 1(b), our two models more accurately predict the peak value of the streamwise Reynolds stress profile while the Vreman model slightly underpredicts it, and the DSM overpredicts the maximum value. In spanwise and wall-normal profiles, the four SGS models show equivalent performance.

	Ma	Re_τ	Re_b	L_x	L_y	L_z	N_x	N_y	N_z	Δx^+	Δy^+	Δz^+
DNS (Foysi *et al.*)	1.50	221	3000	4π	2	$4\pi/3$	192	151	128	14.46	0.84 – 5.02	7.23
LES (Vreman)	1.59	210	2906	12.6	2	4.2	64	152	64	41.42	0.79 – 6.30	13.81
LES (DSM)	1.64	212	2999	12.6	2	4.2	64	152	64	41.76	0.79 – 6.36	13.92
LES (PSA)	1.60	211	2922	12.6	2	4.2	64	152	64	41.46	0.79 – 6.32	13.82
LES (RD-Vreman)	1.62	211	2961	12.6	2	4.2	64	152	64	41.57	0.79 – 6.33	13.86

TABLE 1. Physical and grid parameters for compressible turbulent channel flows at Re_τ = 221 and Ma=1.5.

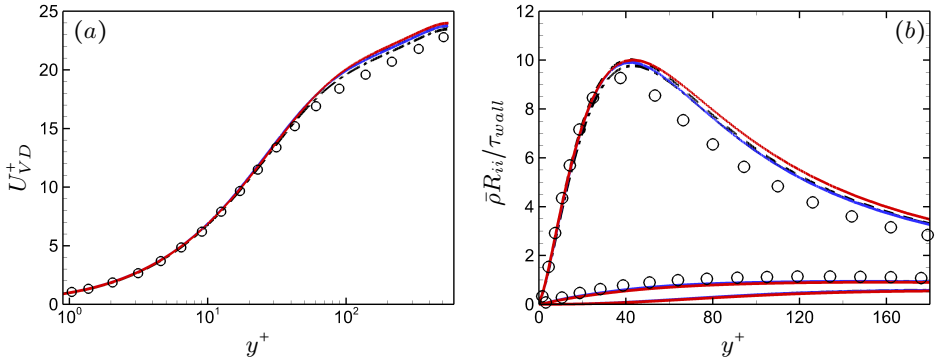

FIGURE 2. (*a*) The Van-Driest transformed mean velocity profiles at Re_τ=556 with Ma=3.0 (*b*) Normalized rms profiles of Favre velocity fluctuations obtained with four SGS models.

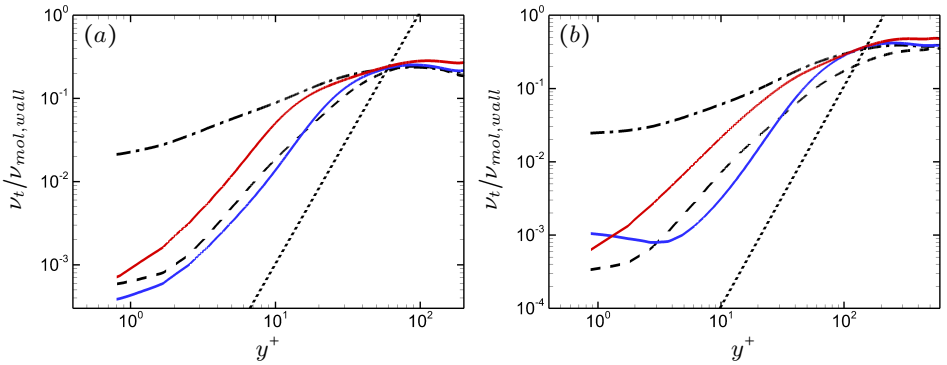

FIGURE 3. (*a*) Mean SGS eddy-viscosity scaled with the wall molecular kinematic viscosity $\nu_{mol,wall}$. — — —, cubic behavior ($\nu_t \sim y^3$); — ·· —, Vreman model; – – –, dynamic Smagorinsky model; —, PSA-model with c_r = 1.3. (*b*) Same as (*a*) but scaled with the wall molecular kinematic viscosity $\nu_{mol,wall}$ at the wall.

3.2. *Compressible turbulent channel flow at Re_τ=556*

To evaluate the performance of the two SGS models in a much coarser grid and a higher Reynolds number flow regime, we also performed LES of compressible turbulent flow at Re_τ = 556 and Ma=3.0. As shown in table 2, the wall-normal grid resolution of the Ma=3.0 case is much coarser than that of the Ma=1.5 case. The friction Reynolds

	Ma	Re_τ	Re_b	L_x	L_y	L_z	N_x	N_y	N_z	Δx^+	Δy^+	Δz^+
DNS (Foysi *et al.*)	3.0	556	6000	4π	2	$4\pi/3$	512	221	256	13.65	$0.89 - 9.38$	8.91
LES (Vreman)	3.29	543	5972	12.6	2	4.2	128	110	96	53.47	$0.87 - 37.70$	23.76
LES (DSM)	3.32	546	6033	12.6	2	4.2	128	110	96	53.67	$0.87 - 37.85$	23.85
LES (PSA)	3.33	549	6045	12.6	2	4.2	128	110	96	53.73	$0.87 - 37.85$	23.88
LES (RD-Vreman)	3.36	549	6092	12.6	2	4.2	128	110	96	54.00	$0.87 - 38.07$	24.00

TABLE 2. Same as table 1 but at $Re_\tau = 556$ and Ma=3.0.

numbers of the LES with the four SGS models show good agreement with the target $Re_\tau = 556$.

As can be shown in figure 2, our two models predict the mean velocity profile as accurately as DSM, but they are slightly overpredicted compared with the mean profile due to the Vreman model. In the profiles of Reynolds stresses, our two models show almost comparable performance with the two established models.

3.3. *Investigation of near-wall behavior*

The analytically constructed near-wall behavior of the PSA-model on the condition of incompressible flows is investigated in the two channel flow cases, Ma=1.5 and 3.0. As shown in figure 3(a), the Vreman model shows the first order dependency of the eddy viscosity with wall-normal distance close to the solid wall in the compressible channel flow at $Re_\tau = 221$. It is notable that our dynamic procedure fixes the inappropriate wall behavior of the Vreman model, namely, from the first order to cubic behavior. Moreover, the PSA-model shows cubic wall behavior in the compressible flow case. Those wall behaviors of the proposed two models are comparable with that of the DSM.

Figure 3(b) displays near-wall behaviors in the compressible channel flows at $Re_\tau = 556$ and Ma=3.0. In this flow configuration, the PSA-model does not guarantee the analytically constructed cubic wall behavior of the SGS eddy viscosity in the Ma=3.0 case. Our restricted assumption on polynomial approximations of the near-wall velocity components may cause the inappropriate behavior. In details, the time derivative term of density in compressible continuity equation may cause the deviation of the SGS eddy-viscosity in the PSA-model from the cubic behavior. Although the PSA-model is not robust to the compressibility effects, the mean SGS eddy viscosity of the PSA model in the viscous sublayer region is about ten times smaller than that of the Vreman model. Moreover, as can be seen in figure 2, the inappropriate wall behavior of the PSA model at $y^+ < 5$ does not have significant effects on turbulence statistics. In contrast to the PSA model, the SGS eddy-viscosity of the RD-Vreman model shows robustness to the compressibility effects.

4. Conclusion

We have completed the validation of two novel SGS eddy-viscosity models by LES of compressible channel flows at $Re_\tau = 221$ and Ma=1.5, and $Re_\tau = 556$ and Ma=3.0, respectively. Comparing turbulence statistics obtained with the proposed models and two established models (DSM and Vreman model), good performance of our two models are recognized. However, further validations on statistically complex flows are required to confirm that the two models have the global applicability to the LES of turbulent flows.

Acknowledgments

Financial support has been provided by the German Research Foundation (Deutsche Forschungsgemeinschaft – DFG) in the framework of the Sonderforschungsbereich Transregio 40.

References

[1] SMAGORINSKY, J. (1963). General circulation experiments with the primitive equations: 1. The basic experiment. *Mon. Weather Rev.*, **91**, 99–164.

[2] VREMAN, A. W. (2004). An eddy-viscosity subgrid-scale model for turbulent shear flow: Algebraic theory and applications. *Phys. Fluids*, **16**, 3670–3681.

[3] NICOUD, F., TODA, H. B., CABRIT, O., BOSE, S. T. AND LEE, J. (2011). Using singular values to build a subgrid-scale model for large eddy simulations. *Phys. Fluids*, **23**, 085106.

[4] GERMANO, M., PIOMELLI, U., MOIN, P. AND CABOT, W. H. (1991). A dynamic subgridscale eddy viscosity model. *Phys. Fluids A*, **3**, 1760–1765.

[5] NICOUD, F. AND DUCROS, F. (1999). Subgrid-Scale Stress Modelling Based on the Square of the Velocity Gradient Tensor. *Flow, Turbulence and Combustion*, **62**, 183–200.

[6] BOSE, S. T. AND MOIN, P. (2010). A class of dynamic mixed models for explicitly filtered LES *CTR Annual Research Briefs*, **62**, 223–236.

[7] LARSSON, J., VICQUELIN, R. AND BERMEJO-MORENO, I (2011). Large eddy simulations of the HyShot II scramjet. *CTR Annual Research Briefs*.

[8] KHALIGHI, Y., NICHOLS, J. W., LELE, S., HAM, F. AND AND MOIN, P. (2011).Unstructured large eddy simulations for prediction of noise issued from turbulent jets in various configurations. *17th AIAA/CEAS Aeroacoustics Conference*, **2886**.

[9] FOYSI, H., SARKAR, S. AND FRIEDRICH, R. (2004). Compressibility effects and turbulence scalings in supersonic channel flow. *J. Fluid Mech.*, **509**, 207–216.